CONTOUR DETECTION IN MRI TAGGED IMAGES USING SHORT-RANGE CORRELATIONS OF DISPLACEMENT FIELDS

B.S. Spottiswoode

MRC/UCT Medical Imaging Research Unit, Department of Human Biology, Faculty of Health Sciences, University of Cape Town, Observatory, 7925, South Africa

Abstract: Magnetic Resonance Imaging (MRI) is fast becoming an indispensable tool for the diagnosis of heart disease. Myocardial tagging is a cardiac MRI technique that allows one to perform a detailed kinematic analysis of the heart muscle. This allows clinicians to non-invasively identify areas of damaged cardiac muscle tissue. Myocardial tagging involves magnetically marking the heart muscle with a set of lines, and monitoring the deformation of these lines as the heart contracts. Harmonic phase (HARP) analysis is a procedure that facilitates the rapid quantification of material displacement and strain from tagged images. There is currently no reliable automated means of outlining the walls of the heart muscle in tagged images. This paper presents a novel method of extracting these contours. The method is based on the fact that the harmonic phase of the heart muscle in a tagged image behaves in an ordered manner over time relative to the enclosed blood and surrounding cavities.

Key words: HARP MRI, myocardial tagging, tissue tracking, segmentation.

1. INTRODUCTION

Heart disease is a leading cause of death in the Western world. In 2000, cardiovascular disease (CVD) caused 39% of deaths in the United States [1], and in 2001 the CVD-related mortality in the United Kingdom was slightly higher than this [2]. CVD is also South Africa's number one killer, being responsible for 19,8% of all deaths each year [3].

Over the past decade, magnetic resonance imaging (MRI) has become a powerful diagnostic tool for heart disease. Myocardial tagging [4] is a cardiac MRI technique that allows one to measure strain and displacement of material points within the heart muscle. The tagging involves using specialised MRI sequences to mark (or *tag*) bands of heart muscle tissue. These tags are material properties of the tissue, and they can be seen to deform as the heart contracts. If the deformation of the tags is monitored, concepts from continuum mechanics can be applied to determine strain and displacement fields, which in turn can be used to identify the strains and wall motion abnormalities associated with a number of heart diseases.

The MRI scanning process can capture a series of tagged images undergoing deformation in a cine format. Two out of the eight frame cine series used in this paper are shown in Figure 1, which gives an example of a tagged image before the heart contracts, at end-diastole, and after the heart has completely contracted, at end-systole. A healthy volunteer was imaged using a Siemens Symphony Quantum 1.5T MRI scanner. The annulus in the centre of Figure 1(b) is the left ventricle (LV), and the crescent-shaped cavity shown on the left of this is the right ventricle (RV). The pulmonary cavity, comprising the left lung in this image, is indicated above and to the right of the heart.

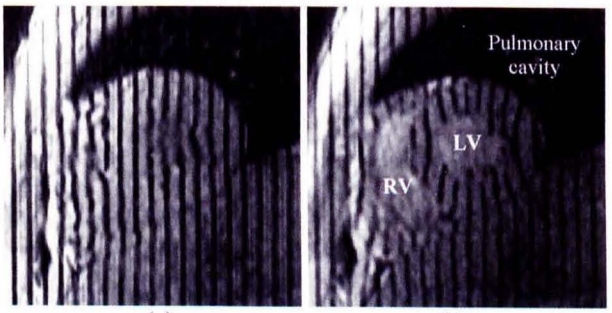

(a) (b)

Figure 1: Example of a tagged image showing the dark bands of saturation (a) undeformed, at end-diastole, and (b) deformed, at end-systole.

These tag lines give an indication of motion and deformation in a direction orthogonal to the lines. A second set of tag lines placed perpendicular to the first, can also be acquired, giving an indication of motion and deformation in two dimensions. It is also possible to investigate motion and deformation in a third dimension, but this requires further imaging planes. As is depicted in Figure 2, the tasks involved in analysing tagged images are typically fourfold:

1. Identify the tag line intersections in each frame of a series of images, and track the motion of these intersections from frame to frame.
2. Represent the behaviour of the heart using a model. This is done in order to quantify the motion of the tagged points from one image to the next in a realisable manner.
3. Generate triangular elements with corners corresponding to the tag intersections. These

triangles can be treated as finite elements and the strain and rigid body displacement can be determined by examining their deformation and displacement respectively.

4. Outline the borders of the heart muscle, or myocardium. This includes both the internal border, or endocardium, and the external border, or epicardium of each ventricle.

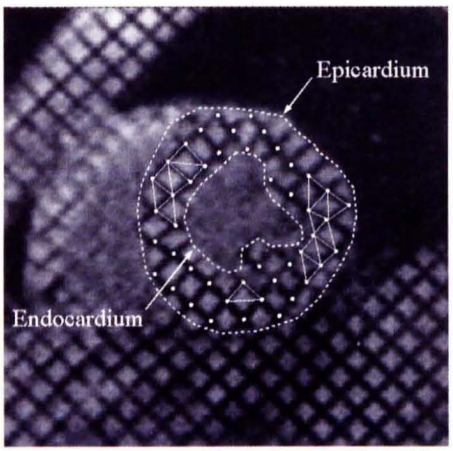

Figure 2: Tagged image of the left ventricle indicating the required image registration.

Recently a technique has been developed for tracking tags based on the concept of harmonic phase (HARP) [5]. The HARP method is completely automated and lends itself to straightforward strain calculations.

It is the last of the above tasks that this paper addresses. Delineating the myocardium accurately is important for a number of reasons. Firstly, clinicians often find it useful to quantify the amount of myocardial wall thickening. Secondly, because of the flow of blood within the ventricles and of air within the lungs, the magnetic resonance (MR) signal of these areas is very noisy. As a result of this, when developing strain maps, the values of strain depicted within the blood and lungs will be completely nonsensical and often elaborately large. A clinician could thus easily be prone to making a misdiagnosis if it is unclear where these borders lie.

This paper proposes a novel method of outlining the myocardium based on excluding areas where the MR signal is behaving in a random fashion, i.e. in fluid-filled areas such as blood and lungs. This is achieved by tracking material points in the images from frame to frame. Points based within stationary tissue or within the myocardium behave in a similar manner to neighbouring points. These points can thus be distinguished from the areas in the blood and lungs by their relatively high short-range correlations. Automating the process of myocardial segmentation is currently one of the final hurdles preventing myocardial tagging from becoming a clinically acceptable methodology.

2. HARMONIC PHASE (HARP) ANALYSIS

Harmonic phase, or HARP, analysis is a fast and elegant technique for processing tagged images. It was first proposed by Osman and Prince [7], and has fuelled a considerable number of research efforts since.

When looking at a tagged image in the Fourier domain, it is seen that the original untagged image is modulated onto a number of spectral peaks, as can be seen in Figure 3(a). These peaks are located at the tag frequency and integer multiples thereof. By filtering out all but one of the two spectra corresponding to the tag frequency, and then performing an inverse Fourier transform, a complex image results. The magnitude of this complex image is merely a crude version of the original untagged image. It can be shown that the phase of this complex image is a material property of the tissue, and can thus be related to myocardial motion and deformation [5, 8]. It is important to note that even though the HARP analysis allows one to track the phase in the HARP images at a sub-pixel resolution, the actual resolution of tracking material points in the myocardium is limited to the tag spacing [6].

2.2. Myocardial tagging

Prior to acquiring a standard cine sequence of the heart, selective excitation can be used to produce a pattern of dark, saturated lines of altered magnetisation. Currently, the most common form of myocardial tagging is the spatial modulation of magnetisation (SPAMM) sequence [4]. Here, the tissue is spatially modulated in a sinusoidal manner, where the dark lines correspond to the troughs of the sinusoids.

A SPAMM sequence is immediately followed by a standard MRI cine sequence. A grid of tag lines can be obtained by applying a further orthogonal SPAMM sequence prior to the cine acquisition. It is important to note that the saturated lines of magnetisation become less distinct with time, a phenomenon known as tag fading. The time constant for this relaxation is 800 ms in myocardium, which is typically sufficient for the tag lines to be visible throughout systole.

2.3. HARP images

Simple SPAMM sequences are described mathematically in [9]. It can be shown from this that, in the Fourier domain, a SPAMM image is the summation of a baseband spectral pattern and a number of sinusoidally modulated patterns at integer multiples of the tag frequency [7].

Let end-diastole be considered to be at time $t = 0$, and let every material point in the heart be marked by its position $\mathbf{p} = [p_1\, p_2]$ at this reference time. As the heart deforms, a material point within the myocardium moves from its reference point $\mathbf{p}$ to a new spatial position $\mathbf{x} = [x_1\, x_2]$ at

time t. This can be characterised by the reference map $\mathbf{p}(\mathbf{x}, t)$. If $I_0(\mathbf{p}(\mathbf{x}, t))$ is the intensity of this material point $\mathbf{p}$ in the absence of the tag pulse sequence, then the application of a SPAMM sequence modifies this intensity according to the relation [10]:

$$I(\mathbf{p}(\mathbf{x},t)) = \sum_{k=1}^{K} I_0(\mathbf{p}(\mathbf{x},t)) c_k(t) e^{j\omega_k^T \mathbf{p}(\mathbf{x},t)} \qquad (1)$$

where the spatial frequencies ω_k are the locations of the spectral peaks, and K, which is a function of the SPAMM sequence, represents the number of spectral peaks present in the Fourier domain. The coefficients c_k are derived from the parameters of the SPAMM sequence, and account for the fading of the tag lines.

The spatial frequency ω_k (in radians per pixel) in the direction perpendicular to the tag lines, has magnitude

$$\omega_k = \frac{2\pi w_c}{N} \qquad (2)$$

where N is the number of pixels spanning the width of the square image, and w_c is the number of pixels between the zero frequency and the centre of the selected spectral peak.

Equation 1 shows that the underlying image is modulated by the SPAMM sequence, and that a SPAMM-tagged image is the sum of K complex harmonic images, each corresponding to a distinct spectral peak identified by the frequency vector ω_k. The spectral peaks in the Fourier domain arise because the sinusoids in the SPAMM tag pattern amplitude modulate (AM) the underlying image, acting as carrier frequencies that shift the underlying spectrum into various positions.

The *displacement field* is defined as the transition from the reference configuration to the current configuration, that is $\mathbf{u}(\mathbf{x}, t) = \mathbf{x} - \mathbf{p}(\mathbf{x}, t)$. Using this relation in the phase component of Equation 1, and another analogy from communications theory, it is seen that Equation 1 represents a phase modulation (PM) of the underlying carrier by a measure of displacement. Thus if the phase of the information that is modulated onto the underlying carrier can be quantified, so can the motion material points within the myocardium.

An estimate of this phase image can be extracted by capturing the spectral peak at the tag frequency using a two dimensional bandpass filter with dimensions large enough to encompass the maximum spreading of the energy around the peak. Note that only one peak out of the symmetric pair is chosen, otherwise there will be phase cancellation. The design of this bandpass filter has been investigated in detail [10, 11]. Performing an inverse Fourier transform on this filtered image will result in a complex image with a phase that depicts the tag positions. Figure 3 shows an estimate of the bandpass filter, as well as both magnitude and phase images of this complex image. Figure 3(d) is the phase image derived from Figure 1(b).

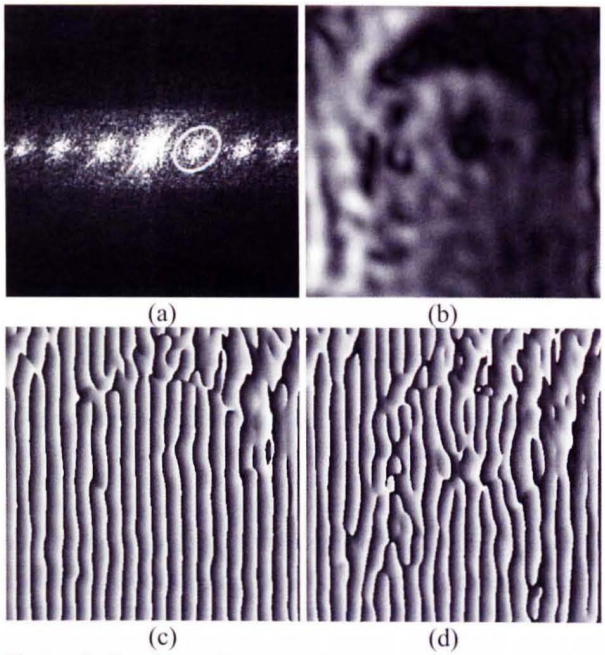

Figure 3: Bandpass filtering of the spectral content of the peak situated at the fundamental tag frequency. (a) The Fourier domain representation of Figure 1(a) and corresponding bandpass filter, (b) the magnitude image, (c) the phase image of the inverse Fourier transform of the filtered image, and (d) the phase image derived from Figure 1(b).

2.4. Displacement fields

The phase in Figure 3(c) and 3(d) is wrapped from -π to π due to the arctan operation. If the images are unwrapped, the motion of each pixel in the image can be uniquely defined in the direction perpendicular to the tag lines. If two such unwrapped images are acquired for orthogonal tagging planes, the two dimensional motion of each point in the image can be uniquely tracked. Unfortunately, these phase images are too noisy to unwrap reliably. However, if the phase images from two successive frames are subtracted from each other, and the motion during this frame duration is less than half the tag spacing, then phase unwrapping can easily be performed.

Assume that two phase images $\phi_{k1}(\mathbf{x}, t)$ and $\phi_{k2}(\mathbf{x}, t)$ have been obtained with linearly independent spatial frequency vectors ω_{k1} and ω_{k2} respectively. The subtraction of two successive frames of phase images gives the wrapped image $\Delta\phi(\mathbf{x}, t_{n'}) = \phi_k(\mathbf{x}, t_{n+1}) - \phi_k(\mathbf{x}, t_n)$, with the unwrapped version being represented as $\Delta\phi_k^*(\mathbf{x}, t_{n'})$. Here n is a discrete frame number and the prime indicates the time segment spanning the frames n to n+1. Thus for a series with F frames, n runs from 1 to F and n' runs from 1 to (F - 1). In the context of this frame subtraction, the displacement field can be more generally defined for each frame pair as $\mathbf{u}(\mathbf{x}, t_{n'}) = \mathbf{u}(\mathbf{x}, t_{n+1}) - \mathbf{p}(\mathbf{x}, t_n)$.

In order to relate $\Delta\phi^*(\mathbf{x}, t_{n'})$ (in grey levels) to $\mathbf{u}(\mathbf{x}, t_{n'})$ (in pixels), two scaling factors are required. Firstly, κ is introduced as the wrapping angle divided by the number of image grey levels. This corresponds to $2\pi/255$ for an 8-bit image. The second constant, which converts radians into pixels, is simply the inverse of the spatial frequency magnitude ω_k, given by Equation 2. Thus the two dimensional displacement $\mathbf{u}_2 = [u_1\ u_2]$ can be calculated according to

$$\mathbf{u}_2(\mathbf{x}, t_{n'}) = \kappa \begin{bmatrix} \Delta\phi^*_{k1}(\mathbf{x}, t_{n'})/\omega_{k1} \\ \Delta\phi^*_{k2}(\mathbf{x}, t_{n'})/\omega_{k2} \end{bmatrix}^T \quad (3)$$

Equation 3 only holds if the motion between frames is less than half the tag spacing, i.e. $|\omega_{ki}\mathbf{u}| < \pi$ for $i = 1, 2$ [10].

Figure 4(a) gives an example of $\Delta\phi^*_{k1}(\mathbf{x}, t_{n'})$ for motion in a horizontal direction. Light pixels indicate motion towards the left and dark pixels indicate motion towards the right. Similarly, Figure 4(b) depicts the corresponding $\Delta\phi^*_{k2}(\mathbf{x}, t_{n'})$ for motion in a vertical direction. Light pixels indicate upwards motion and dark pixels indicate downwards motion. Note the clear radial contraction of the annulus-shaped left ventricle. The displacement field vector plot can easily be derived from these two images.

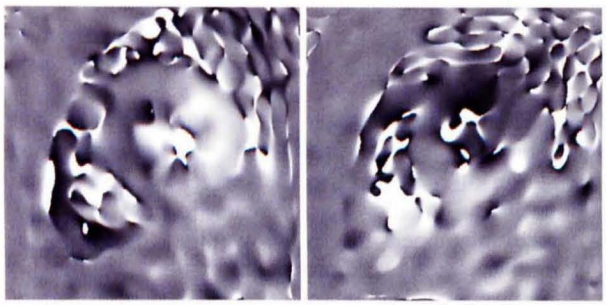

(a) (b)

Figure 4: Images used to construct a displacement field. (a) Motion in the left-right direction. Light pixels depict displacement to the left and dark pixels depict displacement to the right. (b) Motion in the up-down direction. Light pixels depict upwards displacement and dark pixels depict downward displacement.

2.5. Determining strain

Strain can be described as the normalised change of fiber length in a particular direction. Section 2.3 demonstrated that the tag pattern phase is a material tissue property which remains constant despite tag fading. As can be seen by comparing Figure 3(c) to Figure 3(d), it is the gradient of the phase that changes during deformation, doing so in a manner that is inversely proportional to the deformation.

Strain can be calculated directly for each frame using the deformation gradient matrix, which is given by $F(\mathbf{x}, t_n) = \nabla_{\mathbf{x}}\mathbf{p}(\mathbf{x}, t_n)$ where $\nabla_{\mathbf{x}}$ is the gradient with respect to $\mathbf{x}$.

Assume again that two phase images have been obtained with linearly independent spatial frequencies. If $\mathbf{e}=[e_1\ e_2]$ is a unit vector in the image plane, then the strain in the direction of $\mathbf{e}$ is given by [8]:

$$\varepsilon_2(\mathbf{x}, t_n; \mathbf{e}) = \| [\nabla_x \phi(\mathbf{x}, t_n)]^{-1} W\mathbf{e} \| - 1 \quad (4)$$

where $W = diag(\omega_{k1}, \omega_{k2})$ and the Euclidian norm serves to give a scalar value at $\mathbf{p}(\mathbf{x}, t_n)$ in the direction of $\mathbf{e}$. The vectors $\mathbf{e}$ can for example be positioned in a circumferential direction relative to a manually selected point in the centre of the left ventricle.

3. MYOCARDIAL CONTOUR DETECTION

3.1. Overview

The displacement fields and strain maps contain a vast amount of information about the behaviour and condition of the heart in question. Interpretation of these images is however made difficult by the inability to discern the myocardium from the lungs, ventricular blood pools, and other surrounding tissues. The often large random values of strain depicted in the lungs and blood pools could in fact lead to a dangerous misinterpretation of the heart's condition.

A very efficient method of outlining the myocardium was devised by Osman *et al.* [5]. It simply involves performing a thresholding procedure on the magnitude image of the complex Fourier-filtered image, such as that shown in Figure 3(b). The resulting masks are crude and become progressively less accurate with time.

Active contour models have also been used to extract endocardial contours from normal cine cardiac MRI images [12], but an automated method for extracting both epicardial and endocardial contours from tagged images has not been developed.

Immediately after tags are applied, and before the blood in the ventricles has had time to flow out of the imaging plane, the tags show up clearly in the blood pools. This has the implication that the endocardium in the first few frames of a sequence is greatly obscured by the tag lines in the blood, as is clear in Figure 1(a). Image processing methods based on image intensity are completely powerless for these frames. Even marking the myocardium manually, which is currently the method of choice for an accurate outline, is impossible here.

3.2. Short-range correlations of cumulative displacement fields

Cumulative displacement fields: A cumulative displacement field refers to the tracking of material points through an entire sequence by adjoining displacement field vectors end-to-end. For the purposes of this

description, a forward map $\mathbf{x} = \mathbf{x}(\mathbf{p}, t)$ is used instead of the reference map $\mathbf{p} = \mathbf{p}(\mathbf{x}, t)$ used previously. Let $\hat{\mathbf{i}}_1$ and $\hat{\mathbf{i}}_2$ be unit basis vectors for p_1 and p_2 respectively. A forward map gives the present position of the particle that occupied the point $\mathbf{p}$ at time $t = 0$ relative to the referential coordinates $\hat{\mathbf{i}}_1$ and $\hat{\mathbf{i}}_2$. A more detailed description of these maps can be found in any continuum mechanics text.

If all of the reference pixels $\mathbf{p} = [p_1\ p_2]$ lie on a uniform grid at time $t_1 = 0$, then they can be considered to lie on the deformed grid $[x_1(\mathbf{p}, t_n)\ x_2(\mathbf{p}, t_n)]$ at time t_n. The displacement field is described in material coordinates by $\mathbf{u}(\mathbf{p}, t) = \mathbf{x}(\mathbf{p}, t) - \mathbf{p}$. Between two successive frames, this can be adapted to $\mathbf{u}(\mathbf{p}, t_{n'}) = \mathbf{x}(\mathbf{p}, t_{n+1}) - \mathbf{x}(\mathbf{p}, t_n)$. Thus the displacement field vectors for each frame difference $t_{n'}$ originate at the deformed grid position $\mathbf{x}(\mathbf{p}, t_n)$. The cumulative displacement field is shown by plotting $[\mathbf{u}(\mathbf{p}, t_{1'}), \ldots, \mathbf{u}(\mathbf{p}, t_{(F-1)'})]$ on the same axes. Here F is the number of frames in the cine series. Figure 5 shows the cumulative displacement field for the eight frame sequence used in this study. The contraction of the left ventricle is depicted very clearly. Note that the vector density has been reduced tenfold for display purposes.

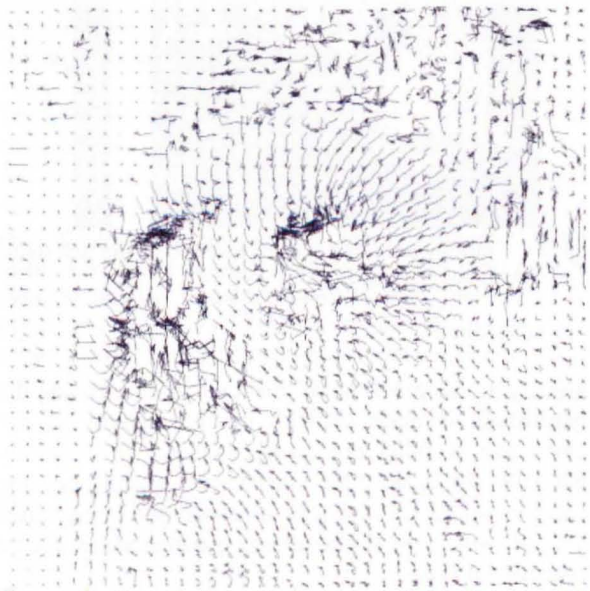

Figure 5: Cumulative displacement field for an eight frame sequence.

Myocardium mask based on short-range correlations: A striking feature in Figure 5 is the chaotic behaviour of the cumulative displacement vectors in the pulmonary cavity and blood pools. In the pulmonary cavity, this is because no tags can be placed in spaces containing air and hence any readings of harmonic phase can simply be classified as noise. The tags initially placed in the blood pools are washed away as blood is ejected from the ventricles, resulting in similar nonsensical harmonic phase readings for these areas.

It is proposed here that the chaotic behaviour of the lungs and blood pools versus the more ordered behaviour of the myocardium be used as a means of differentiating between these areas. One way of achieving this is to identify short range correlations between the vector components making up the cumulative displacement fields.

This can be done here by calculating spatial derivatives on the vector components for all the frames of a series. Vectors behaving in a manner similar to their neighbours will have low spatial derivatives, whereas random behaviour will result in higher values.

The cumulative displacement field can be thought of as two sets of three dimensional matrices containing the spatiotemporal coordinates $\mathbf{x}(p_1, t_n)$ and $\mathbf{x}(p_2, t_n)$ respectively, for all images $n = 1, \ldots, F$. One matrix thus contains coordinates for the $\hat{\mathbf{i}}_1$ direction, and the other contains coordinates for the $\hat{\mathbf{i}}_2$ direction. Note that the two sets of two dimensional matrix entries corresponding to t_1 simply describe the initial grid point coordinates. The corresponding entries for the latter frames describe the coordinates of these (deformed) grid points at these frames. The pair of three dimensional matrices thus portrays the motion of the material area described by each image pixel throughout the entire cine series. Using this representation, any data analysis performed on a set of coordinates through all time frames of a series can be mapped to the original position on thefirst frame.

The myocardium mask for the first frame of a sequence can be obtained by calculating

$$M(\mathbf{x}(p_k, t_1)) \approx \sum_{n'=1}^{F-1} \left[\left(\frac{\partial \mathbf{u}(p_k, t_{n'})}{\partial \hat{\mathbf{i}}_1} \right)^2 + \left(\frac{\partial \mathbf{u}(p_k, t_{n'})}{\partial \hat{\mathbf{i}}_2} \right)^2 \right] \quad (5)$$

for $k = 1, 2$, and summing $M(\mathbf{x}(p_1, t_1))$ and $M(\mathbf{x}(p_2, t_1))$. In summary, the spatial derivatives with respect to both $\mathbf{u}(p_1, t_{n'})$ and $\mathbf{u}(p_2, t_{n'})$ are taken in both $\hat{\mathbf{i}}_1$ and $\hat{\mathbf{i}}_2$ directions. The results are squared and summed for all $(F - 1)$ frame differences.

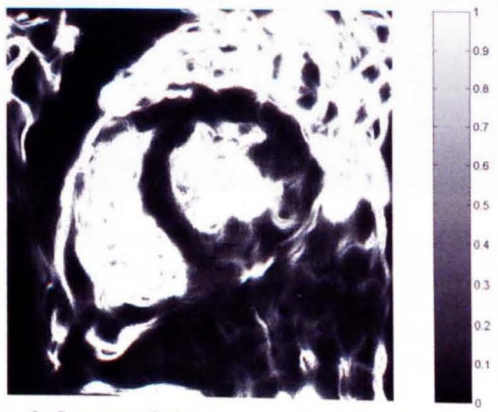

Figure 6: Image of the myocardium for the first frame based on performing spatial derivatives on the vector components for all the frames of a series.

Figure 6 is the image that results when applying this method to the full-resolution version of the cumulative displacement field data set presented in Figure 5. A simple smoothing and thresholding procedure can be applied to this image to give a mask of the myocardium that can be used as a canvas for the strain map of the first frame. The distinction between myocardium and blood/lung is typically large enough to make the threshold level relatively unimportant.

Tracking and error analysis: Tracking the myocardium mask from t_1 through to t_F is easily done given the two sets of three dimensional matrices of $\mathbf{x}(\mathbf{p}, t_n)$. Because the displacement fields are calculated to a sub-pixel resolution, rounding artifacts appear as stretch lines on the subsequent masks. These can easily be removed by scanning the image for small blocks of non-myocardium sandwiched between myocardium, and labelling these as myocardium. Figure 7 shows the myocardium outlines superimposed onto a summation of vertical and horizontal tagged images for four out of the eight frames of the sequence. Note that the myocardium outline is completely invisible to the human eye for the first frame, when the tag lines appear in the blood pools. The accuracy of tracking points using a cumulative displacement field is calculated by comparing the phase coordinates at $t_1 (= 0)$ with those at t_F.

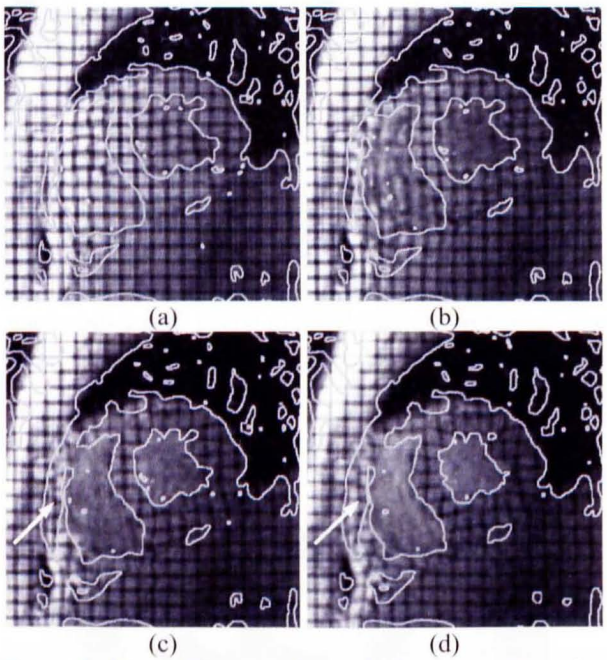

Figure 7: Myocardium mask overlaid onto a summation of vertical and horizontal tagged images. (a) Frame 1, (b) frame 3, (c) frame 5, and (d) frame 7. The arrows indicate an 'additional' tag line that has arisen because of motion perpendicular to the image plane.

The slope of the harmonic phase image at t_F in the directions $\hat{\mathbf{i}}_1$ and $\hat{\mathbf{i}}_2$ is used to give an estimate of the tracking error in pixels. This tracking error is depicted in Figure 8. It is interesting to note that the tracking error of the areas exhibiting chaotic behaviour is far higher than that of the myocardium, adding further evidence to the random nature of the harmonic phase in the lungs and blood pools. For the data set presented in this paper, the mean tracking error and standard deviation are 4.52 and 5.00 pixels respectively for the entire image, and 1.42 and 2.26 pixels respectively for the myocardium (as defined by the spatial derivative mask). The processing time required to calculate the full 464 by 464 pixel cumulative displacement field for eight frames was 109 seconds on a 1.6 GHz Pentium 4, with a further minute being required to calculate the eight myocardium masks. A more accurate method for tracking harmonic phase coordinates from frame to frame has also been developed [5]. This method involves using a Newton-Raphson iterative procedure to locate the closest set of identical harmonic phase coordinates in the subsequent frame. The accuracy obtained is about 0.1 to 0.2 pixels, but the processing time would amount to over an hour for this data set [5].

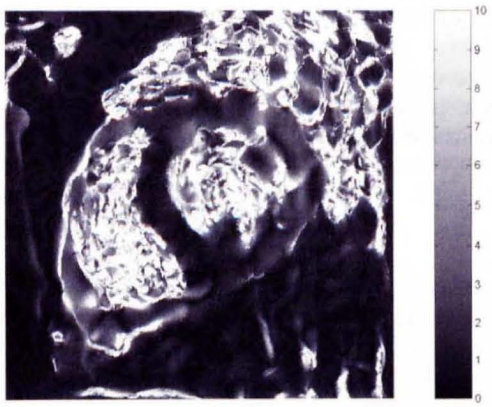

Figure 8: Tracking error in pixels, represented on the first frame of an eight frame sequence.

4. DISCUSSION

Quantifying the precision of this method of outlining the myocardium is made difficult by the inability of the human eye or other processing methods to accurately undertake the task. One method of quantifying the precision would be to acquire a normal MRI cine series with the same spatial and timing parameters as a cine sequence with tags.

A shortcoming of the two dimensional HARP technique presented here is that it applies only for apparent motion, i.e. motion in the plane of the image. Motion perpendicular to the plane of the image can not be detected, and only the component in the plane of the image is portrayed on the displacement field. For a mid-ventricular view of the left ventricle, this is not very problematic, since the motion perpendicular to the plane of the image is fairly uniform throughout the left ventricle [10].

The motion of the right ventricle is not this simple, and a three dimensional analysis would be required for an accurate study. The arrows in Figure 7(c) and 7(d)

indicate a tag line that has moved into the image due to out-of-plane motion. This has resulted in a large portion of the right ventricle that has not been identified. The three dimensional application of both HARP and this new contour detection will be the focus for future work in this area.

5. CONCLUSION

Despite the fact that the concept of myocardial tagging was developed almost fifteen years ago, it has still not found its way into a routine clinical environment. Over a decade of extensive research has honed the tagged image processing techniques, and a complete strain analysis is now a relatively fast and accurate procedure.

Delineating the myocardium using methods based on pixel intensities is not a trivial task, and no acceptable methods have evolved. The development of a suitable method would be an important step towards the routine clinical use of myocardial tagging for the analysis of cardiac strain.

Cardiac strain maps have the important potential application of assisting in the diagnosis of ischaemic heart disease, which is a leading cause of mortality in the Western world. Ischaemic areas of myocardium do not contract properly, and display distinct strain patterns.

The segmentation method introduced in this paper uses short range correlations on cumulative displacement fields to discern between the myocardium and its adjacent cavities. The processing times for the technique are reasonable. The technique also identifies the myocardium in the first few frames, a task that had not been possible using techniques based on image intensity because of the presence of tag lines in the ventricular blood pools. The accuracy of the method still needs to be verified on normal cine images.

6. REFERENCES

[1] American Heart Association website, 2003. http://www.americanheart.org. Accessed September 2003.

[2] British heart foundation statistics website, 2003. http://www.heartstats.org. Accessed May 2003.

[3] The Heart Foundation of South Africa website, 2003. http://www.heartfoundation.co.za. Accessed September 2003.

[4] L. Axel and L. Dougherty: "MR imaging of motion with spatial modulation of magnetization." *Radiology* Vol. 171: pp. 841–845, 1989.

[5] N.F. Osman, W.S. Kerwin, E.R. McVeigh, J.L. Prince: "Cardiac motion tracking using cine harmonic phase (HARP) magnetic resonance imaging. *Magnetic Resonance in Medicine* Vol. 42, pp. 1048–1060, 1999.

[6] V. Parthasarathy and Prince J.L.: "Strain resolution from HARP-MRI." *Proceedings of the International Society of Magnetic Resonance in Medicine (ISMRM), Kyoto, Japan, 2003.*

[7] N.F. Osman and J.L. Prince: "Direct calculation of 2D components of myocardial strain using sinusoidal MR tagging" *Proceedings of SPIE Medical Imaging: Image Processing Conference, San Diego, California*, 1998.

[8] N.F. Osman and J.L. Prince: "Angle images for measuring heart motion from tagged MRI" *Proceedings of the International Conference on Image Processing (ICIP), Chicago, Illinois, USA*, pp. 704–708, 1998.

[9] J.L. Prince and E.R. McVeigh: "Motion estimation from tagged MR image sequences" *IEEE Transactions on Medical Imaging* Vol. 1, No. 2, pp. 238–249, 1992.

[10] N.F. Osman and J.L. Prince: "Imaging heart motion using harmonic phase MRI" *IEEE Transactions on Medical Imaging* Vol. 19, No. 3, pp. 186–202, 2000.

[11] N.F. Osman and J.L. Prince: "On the design of the bandpass filters in harmonic phase MRI" *Proceedings of the International Conference on Image Processing (ICIP), Vancouver, Canada*, 2000.

[12] S. Ranganath: "Contour extraction from cardiac MRI studies using snakes" *IEEE Transactions on Medical Imaging* Vol. 14, No. 2, pp. 328–338, 1995.